

## 02 Spectroscopic investigation of structural and magnetic properties of $\text{TbCr}_3(\text{BO}_3)_4$

© N.N. Kuzmin<sup>1,2,3</sup>, K.N. Boldyrev<sup>1,3</sup>, V.V. Maltsev<sup>2</sup>

<sup>1</sup> Institute of Spectroscopy, Russian Academy of Sciences, 108840 Troitsk, Moscow, Russia

<sup>2</sup> Lomonosov Moscow State University, 119991 Moscow, Russia

<sup>3</sup> Moscow Institute of Physics and Technology (National Research University), 141700 Dolgoprudny, Moscow Region, Russia

e-mail: kolyanfclm@gmail.com

Received September 05, 2021

Revised September 15, 2021

Accepted September 22, 2021

The paper presents a flux crystal growth technique, studies of the structural peculiarities and the optical absorption spectra of double orthoborate  $\text{TbCr}_3(\text{BO}_3)_4$  with a huntite structure. The intensities of the phonon modes were used to determine the ratios of the rhombohedral and monoclinic polytypes for this compound, depending on the growth conditions. The broadband absorption spectra of the  $\text{Tb}^{3+}$  ions in  $\text{TbCr}_3(\text{BO}_3)_4$  single crystals were studied in the temperature range from room temperature to 3.0 K. From them, the energies of the crystal-field levels of the  $\text{Tb}^{3+}$  ion were determined. The temperature dependence of the absorption spectra of the  $\text{Er}^{3+}$  probe ion in  $\text{TbCr}_3(\text{BO}_3)_4:\text{Er}(1\%)$  shows that there are two phase transitions and agrees with their previously proposed interpretation: at 8.8 K, the chromium subsystem antiferromagnetically orders, and at 5 K, a reorientation of chromium magnetic moments occurs.

**Keywords:** rare-earth chromium borates, magnetic ordering, polytypes, crystal growth, optical spectroscopy.

DOI: 10.21883/EOS.2022.01.52988.30-21

### Introduction

Borates have a wide variety of structures and have proven themselves as functional materials [1–3]. The diversity of their crystal structures is explained primarily by the existence of two types of boron coordination polyhedrons —  $\text{BO}_3$ -triangles and  $\text{BO}_4$ -tetrahedra prone to polymerization according to various laws and the formation of superstructural groups. Borates are applied in optical systems [2,4–7], as well as fire retardants [8], molecular sieves [9] and solid electrolytes [10]. In terms of commercial use, borates have the greatest potential for applications as new optical materials, they are non-linear optical media for sources of ultraviolet (UV) and deep UV radiation [2,4–6], birefringent materials [11] and the active medium of lasers with self-doubling and self-mixing frequencies [12]. Many borates have non-centrosymmetric structures, wide spectral windows, good chemical stability, mechanical strength [2,4–6,13–15]. Crystals of such borates as  $\text{KB}_5\text{O}_8 \cdot 4\text{H}_2\text{O}$ ,  $\text{LiB}_3\text{O}_5$ ,  $\beta\text{-BaB}_2\text{O}_4$ ,  $\text{CsB}_3\text{O}_5$ ,  $\alpha\text{-BiB}_3\text{O}_6$ ,  $\text{CsLiB}_6\text{O}_{10}$ ,  $\text{KB}_2\text{BO}_3\text{F}_2$  and  $\text{Sr}_2\text{Be}_2\text{B}_2\text{O}_7$  are promising non-linear optical materials [3,16–22];  $\text{Ca}_3(\text{BO}_3)_2$ ,  $\alpha\text{-BaB}_2\text{O}_4$ ,  $\text{Ba}_2M(\text{B}_3\text{O}_6)_2$  ( $M = \text{Mg}$  and  $\text{Ca}$ ),  $\text{Ba}_3\text{Y}(\text{B}_3\text{O}_6)_2$  and  $\text{Ca}(\text{BO}_2)_2$  serve as promising birefringent materials for light polarization in deep UV range spectrum [23–28]. Borates  $\text{YAl}_3(\text{BO}_3)_4$ ,  $\text{RMgB}_5\text{O}_{10}$  ( $R = \text{La}$ ,  $\text{Gd}$ ),  $\text{RCa}_4\text{O}(\text{BO}_3)_3$  ( $R = \text{Y}$ ,  $\text{Gd}$ ),  $\text{La}_2\text{CaB}_{10}\text{O}_{19}$  [29–31], activated by rare-earth (RE) ions, can be used as active media for lasers.

The double borates containing ions of REE and 3d-metals in their structure are of considerable interest. This is

determined by the fact that such compounds can have interesting magnetic properties due to two magnetic subsystems presence [32]. These include an extensive family of huntite-like borate compounds. It is known that in rare-earth ferrobates  $\text{RFe}_3(\text{BO}_3)_4$  ( $R = \text{Y}$ ,  $\text{La}$ – $\text{Yb}$ ) the magnetic subsystem of iron is antiferromagnetically ordered at temperatures of about 40 K, with the formation of various magnetic structures that depend on the RE ion. In the paper [33] it was shown that  $\text{GdFe}_3(\text{BO}_3)_4$  refers to class of multiferroics of II type. In  $\text{NdFe}_3(\text{BO}_3)_4$  [34] and  $\text{SmFe}_3(\text{BO}_3)_4$  [35] a large magnetoelectric effect is observed. Such physical properties make these compounds promising in terms of possible practical applications.

On the contrary, RE chromium borates  $\text{RCr}_3(\text{BO}_3)_4$  ( $R = \text{La}$ – $\text{Er}$ ) are underexplored. It was shown in the papers [36,37] that RE chromium borates are characterized by two structural modifications: rhombohedral (space group (sp. gr.)  $R32$ ) and monoclinic (sp. gr.  $C2/c$ ), which in many cases coexist in one crystal, and their ratio depends on the RE ion, the concentration of the initial components in the melt, and the crystal growth conditions [37,38]. Both crystal structures consist of three types of coordination polyhedrons:  $\text{RO}_6$  trigonal prisms,  $\text{CrO}_6$  octahedrons, and  $\text{BO}_3$  triangles.  $\text{CrO}_6$  octahedrons are interconnected by edges and form helical chains along  $c$  axis; distorted trigonal prisms of RE element (REE) ions are located between these chains and are isolated from each other. RE chromium borates with La [39], Nd [40], Sm [41], Eu [42], Gd [43–45], Tb [46], Dy [47] are ordered antiferromagnetically with Neel

temperature  $T_N$  in range of temperatures 6.5–10 K. There are few papers on the synthesis of these compounds [37,46].

In the present paper the absorption spectra of terbium-chromium borate crystals in the far infrared (IR) region were obtained. According to these spectra the dependence of the ratio of polytype modifications with sp.gr.  $R32$  and  $C2/c$  on growing conditions was revealed. The temperatures of magnetic phase transitions in the rhombohedral polytype  $\text{TbCr}_3(\text{BO}_3)_4$  are determined by the erbium spectroscopic probe method. The paper also presents a diagram of the Stark energy levels of the  $\text{Tb}^{3+}$  ion in  $\text{TbCr}_3(\text{BO}_3)_4$  in the paramagnetic state.

## Experimental part

### Growing terbium-chromium borate crystals

Terbium-chromium borate crystals with a size of about  $0.5 \times 0.5 \times 0.5$  mm were grown by spontaneous crystallization from a complex solution-melt based on the data of its stability field in a pseudobinary system  $\text{TbCr}_3(\text{BO}_3)_4\text{--K}_2\text{Mo}_3\text{O}_{10}$  [46].

In growth experiments monitoring and regulation of temperature in vertical furnaces with a fechral heater were carried out by Proterm-100 temperature controllers with Pt/Rh–Pt-thermocouplings (calibration PP10). The accuracy of the temperature maintenance in the working zone of the furnace was usually  $\pm 0.1^\circ\text{C}$ . The solvent ( $\text{K}_2\text{Mo}_3\text{O}_{10}$ ) content varied in the range of 10–60 wt.%. Initial components of charge  $\text{Tb}_4\text{O}_7$ ,  $\text{Cr}_2\text{O}_3$ ,  $\text{B}_2\text{O}_3$ ,  $\text{K}_2\text{MoO}_4$  and  $\text{MoO}_3$  (qualification not below „chem. pure“) were placed in platinum crucibles 10 ml and heated up to  $1130^\circ\text{C}$ . Then, for 24 h, the melt was kept at this temperature for homogenization. Then it was cooled at a rate of  $1^\circ\text{C/h}$  to  $900^\circ\text{C}$ , after which its temperature rapidly dropped to  $300^\circ\text{C}$ . At the end of the growth process the crucible was removed from the furnace, and the crystals were removed from the potassium trimolybdate by dissolving it in concentrated hydrochloric acid.

To study magnetic phase transitions in  $\text{TbCr}_3(\text{BO}_3)_4$  the crystals doped with 1% Er were obtained. The size of such crystals was up to  $0.1 \times 0.1 \times 0.1$  mm. In this experiment the composition of the initial charge contained 50 wt.%  $\text{TbCr}_3(\text{BO}_3)_4\text{:Er}(1\%)$  and 50 wt.%  $\text{K}_2\text{Mo}_3\text{O}_{10}$ , since at other ratios of charge and solvent the crystals doped with erbium were not obtained.

The primary identification of the grown crystals was carried out on an XCalibur S CCD single crystal diffractometer and a DRON-3M powder diffractometer.

### Optical spectroscopy of terbium-chromium borate

Absorption spectra of unoriented crystals of terbium-chromium borate in the near-IR range, as well as of powder material  $\text{TbCr}_3(\text{BO}_3)_4\text{:Er}(1\%)$  in the near-IR range, and  $\text{TbCr}_3(\text{BO}_3)_4$  in the far- and mid-IR ranges were recorded on Bruker IFS 125HR Fourier spectrometer. To obtain the spectra of the powder material the method of preparing pressed tablets was used. At measurements

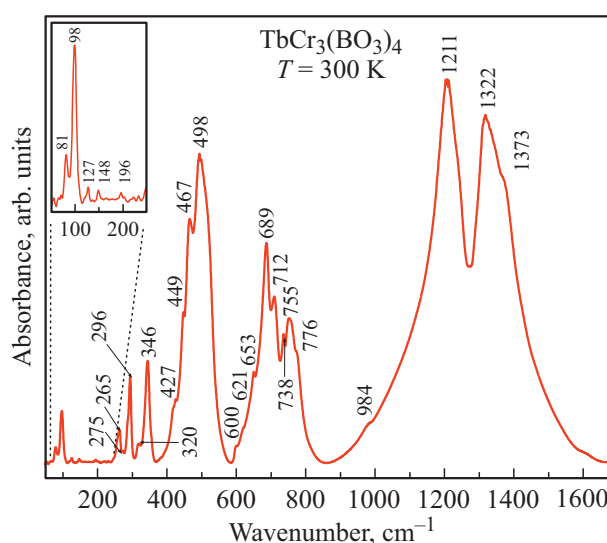


**Figure 1.** Panoramic phonon absorption spectrum of  $\text{TbCr}_3(\text{BO}_3)_4$  at room temperature.

in range of  $20\text{--}600\text{ cm}^{-1}$  the polycrystalline powder  $\text{TbCr}_3(\text{BO}_3)_4$  with weight  $\sim 2$  mg was ground in corundum poulder with  $\sim 50$  mg of polyethylene; at measurements in ranges of  $400\text{--}1700$  and  $2000\text{--}12000\text{ cm}^{-1}$  sample was prepared in similar way from  $\sim 5$  mg  $\text{TbCr}_3(\text{BO}_3)_4$  and  $\sim 40$  mg  $\text{TbCr}_3(\text{BO}_3)_4\text{:Er}(1\%)$ , respectively, and  $\sim 200$  mg KBr. The mixtures were then placed in a mold and pressed into a tablet. Absorption spectra in the far-IR range were obtained at room temperature with a resolution of  $2\text{ cm}^{-1}$ ; in the mid- and near-IR ranges the spectra were obtained with a resolution of up to  $0.1\text{ cm}^{-1}$  and in the temperature range of  $3.0\text{--}300$  K. Low-temperature measurements were carried out using a Sumitomo SRP-082 closed cycle cryostat. The temperature was monitored by a Lakeshore 335 controller with a silicon thermal diode, which makes it possible to measure temperatures in the range of  $1.8\text{--}350$  K with an accuracy of  $\pm 0.1$  K.

## Results and discussion

Figure 1 shows the panoramic phonon absorption spectrum of terbium-chromium borate obtained at charge composition 50 wt.%  $\text{TbCr}_3(\text{BO}_3)_4$  and 50 wt.%  $\text{K}_2\text{Mo}_3\text{O}_{10}$ , in the range of  $50\text{--}1650\text{ cm}^{-1}$  at room temperature. Such spectrum is characteristic for the entire family of borates with the huntite structure [36,37,46]. In RE chromium borates two polytype modifications with sp.gr.  $R32$  and  $C2/c$  were detected. It was shown in the paper [48] for  $\text{GdCr}_3(\text{BO}_3)_4$  that the main differences in the absorption spectra of these modifications are observed in the far-IR range. Thus, the monoclinic modification, in contrast to the rhombohedral one, has absorption bands  $\sim 73$ ,  $126$ ,  $148$ ,  $248$ ,  $275\text{ cm}^{-1}$ . The same paper describes a method for determining their number from the ratio of intensities of phonon modes  $\sim 73$  and  $\sim 79\text{ cm}^{-1}$

**Table 1.** The ratio of rhombohedral and monoclinic polytypes in  $\text{TbCr}_3(\text{BO}_3)_4$  crystals at different borate-to-solvent ratios in charge

Ratio of borate to solvent in the charge	Ratio of modifications with pr. gr. $R32$ and $C2/c$
40:60	97:3
50:50	95:5
60:40	70:30
70:30	75:25
80:20	90:10
90:10	60:40

(translational vibrations of the  $\text{Gd}^{3+}$  ion in modifications with sp.gr.  $C2/c$  and  $R32$ , respectively). These modes in  $\text{TbCr}_3(\text{BO}_3)_4$  correspond to oscillations at frequencies  $\sim 71$  and  $\sim 81 \text{ cm}^{-1}$ . According to this method the content of polytypes in the grown crystals was estimated. The spectra in the far-IR region are shown in Fig. 2, and the results of determining the ratio of polytypes — in the Table 1.

From the Table 1 it follows, that at a monotonic decreasing of the solvent amount and the corresponding proportional increasing of the crystallized substance fracture in the solution-melt, the amount of the higher-temperature phase with sp.gr.  $C2/c$  increases [49], which is easily explained by the crystallization temperature increasing under these conditions. However, after a certain value the amount of phase with sp.gr.  $R32$  increases again, and in such experiments incomplete melting and weak decrystallization of the initial charge were observed. Most likely, in this case the formation of the monoclinic modification of  $\text{TbCr}_3(\text{BO}_3)_4$  occurred from a small amount of solution-

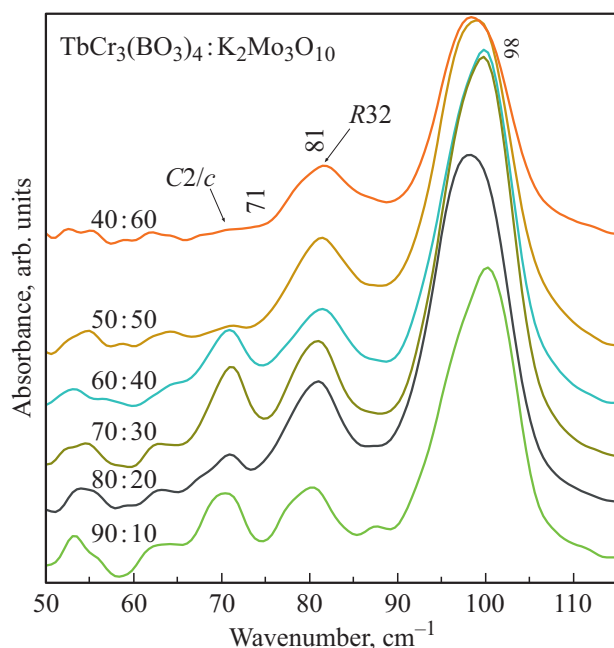


**Figure 2.** Absorption spectra of terbium-chromium borate in far-IR range at different ratios of borate-to-solvent in charge.

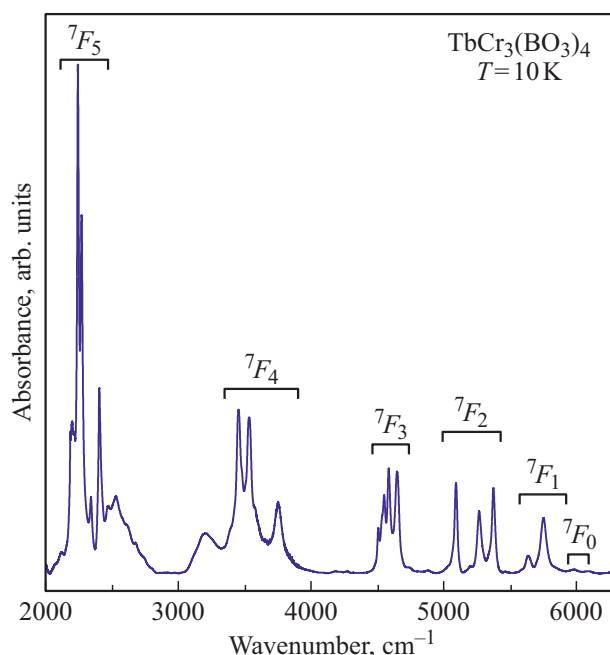


**Figure 3.** Absorption spectrum of the  $\text{Tb}^{3+}$  ion in the paramagnetic state of  $\text{TbCr}_3(\text{BO}_3)_4$  crystal at temperature of 10 K

melt locally formed in the general volume of the unmelted charge, while the rhombohedral modification of this borate was synthesized with a sufficiently long cooling according to the principle of a solid-phase reaction. A similar mechanism of phase formation in multicomponent systems was observed earlier by the authors in the paper [50].

In addition to the phonon spectra, the absorption spectra were obtained in the range of electronic transitions in the  $\text{Tb}^{3+}$  ion. Figure 3 shows the absorption spectrum of the  $\text{Tb}^{3+}$  ion in terbium-chromium borate crystals at temperature of 10 K. It consists of relatively narrow lines corresponding to optical transitions between energy levels in  $4f^8$ -shell of the  $\text{Tb}^{3+}$  ion. This ion has several multiplets in the IR region, above  $15000 \text{ cm}^{-1}$  wide absorption bands are observed in the spectra, due to  $\text{Cr}^{3+}$  ions, which makes it difficult to detect  $^5D_4$  multiplet. Note that for the crystals under study the number of main lines in the low-temperature absorption spectra does not exceed the maximum possible number for one absorbing center, which together with the similarity to the absorption spectra of the  $\text{Tb}^{3+}$  ion in terbium ferroborate with the huntite structure [51] indicates a significant predominance of the rhombohedral modification over the monoclinic one.

The crystal field, depending on its symmetry, completely or partially removes the degeneracy of the energy levels of the free ion with integer spin. For example, crystal field of symmetry  $D_3$  splits the level  $^7F_6$  of free ion  $\text{Tb}^{3+}$  into nine sublevels. At low temperatures the excited levels of the ground multiplet  $^7F_6$  of the terbium ion are not populated, which makes it possible to determine the energies of the levels of the excited multiplets in this

**Table 2.** Energy ( $E$ ) of Stark levels of  $\text{Tb}^{3+}$  in paramagnetic  $\text{TbCr}_3(\text{BO}_3)_4$ 

$E, \text{cm}^{-1}$	$^{2S+1}L_J$
0; 203; 250	$^7F_6$
2183; 2196; 2213; 2240; 2268; 2339; 2402	$^7F_5$
3451; 3532; 3576; 3752	$^7F_4$
4505; 4532; 4549; 4583; 4647	$^7F_3$
5091; 5265; 5373	$^7F_2$
5635; 5751	$^7F_1$
5981	$^7F_0$

ion from the optical spectra. Thus, the energy levels of the excited multiplets  $\text{Tb}^{3+}$  were obtained from the low-temperature absorption spectra, and three energy levels of the main multiplet were determined from the temperature dependence of the absorption spectra (Fig. 4, *a*, Table 2). Note that some spectral lines have an asymmetric shape, for example, all lines of  $^7F_2$  multiplet of the  $\text{Tb}^{3+}$  ion in  $\text{TbCr}_3(\text{BO}_3)_4:\text{Er}(1\%)$ . At low temperatures the contour of such lines turns into a main line and a satellite (Fig. 4, *b*). Such satellites are shifted to the high-frequency side from the main line by 8–35  $\text{cm}^{-1}$ . Similar satellites were encountered earlier in  $\text{TbFe}_3(\text{BO}_3)_4$  [51], where their appearance was associated with optical  $f-f$ -transitions in the  $\text{Tb}^{3+}$  ions near lattice defects, which were impurities of molybdenum and bismuth. These impurities entered the crystal structure from the solvent during crystal growth. The larger number of satellites in  $\text{TbCr}_3(\text{BO}_3)_4:\text{Er}(1\%)$  is explained by the fact that during its growth potassium trimolybdate was used as solvent, in which  $\text{MoO}_3$  is not bonded to  $\text{Bi}_2\text{O}_3$  [52], and the erbium impurity is also important (because  $\text{TbCr}_3(\text{BO}_3)_4$  has fewer such satellites).

The study of magnetic phase transitions in  $\text{TbCr}_3(\text{BO}_3)_4$  was carried out using the erbium spectroscopic probe method. Rare-earth spectroscopic probing is most often used to solve structural chemistry problems to determine the nearest environment of the coordination center [53]. In M.N. Popova's group the same method (using  $\text{Er}^{3+}$  ion as a probe) was used to study magnetic phase transitions and determine magnetic structures. With its help such compounds as  $\text{R}_2\text{Cu}_2\text{O}_5$ ,  $\text{R}_2\text{BaCuO}_5$ ,  $\text{R}_2\text{BaNiO}_5$ ,  $\text{RFe}_3(\text{BO}_3)_4$  ( $R = \text{Y}$ ,  $\text{La-Lu}$ ) were studied [54–62]. On Fig. 5, *a* the absorption spectrum of paramagnetic  $\text{TbCr}_3(\text{BO}_3)_4:\text{Er}(1\%)$  in region of transition  $^4I_{15/2} \rightarrow ^4I_{13/2}$  in the  $\text{Er}^{3+}$  ion is shown. In crystal field with symmetry below cubic the energy levels of free ion with an odd number of electrons (which is the  $\text{Er}^{3+}$  ion) split into Kramers doublets in accordance with the formula  $(2J+1)/2$ , where  $J$  is total angular moment of electrons. Thus, in terbium-chromium borate, where the  $\text{Er}^{3+}$  ion occupies a position with  $D_3$  symmetry, 8 Stark sublevels for the main multiplet  $^4I_{15/2}$  and 7 for the multiplet  $^4I_{13/2}$  are formed.

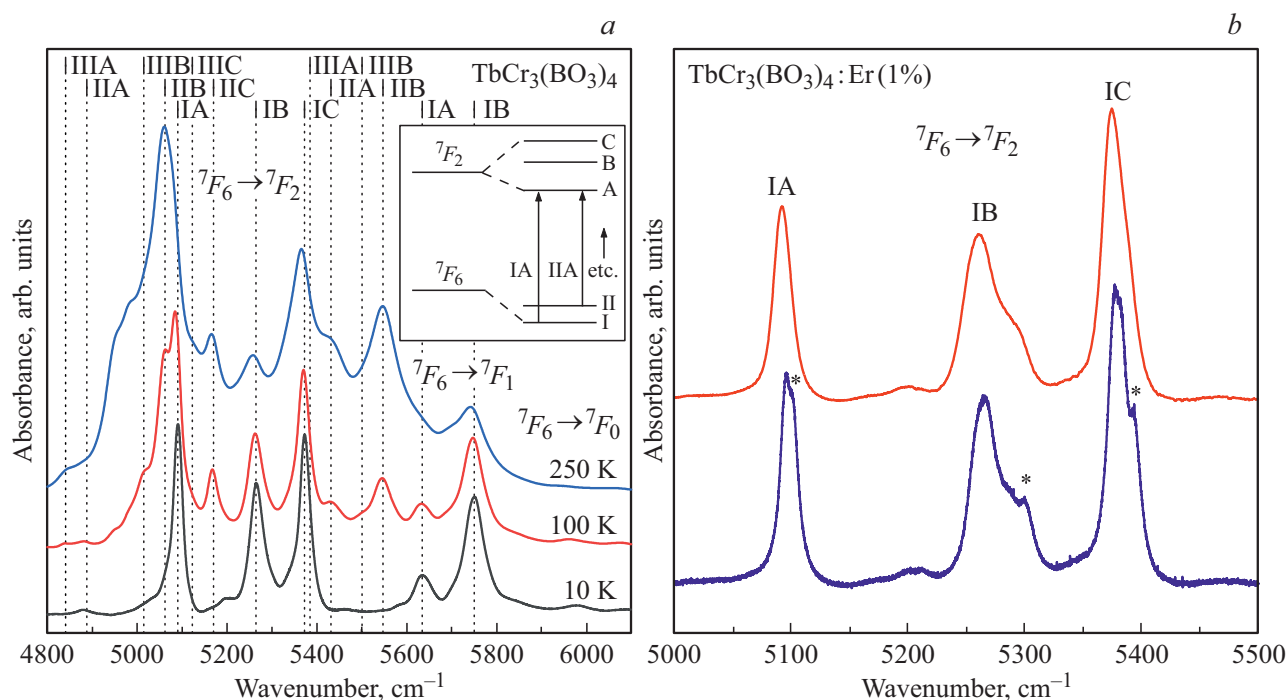
In the absence of the magnetic field the Kramers doublets remain doubly degenerate, and this degeneracy cannot

be removed by any perturbation other than the magnetic field. The appearance of a magnetic field, external or internal (arising during the magnetic ordering of the crystal), removes the Kramers degeneracy, and the corresponding spectral line is split into maximum four components (see the diagram in Fig. 5, *c*). The described splitting of spectral lines is an indicator of magnetic ordering in the system.

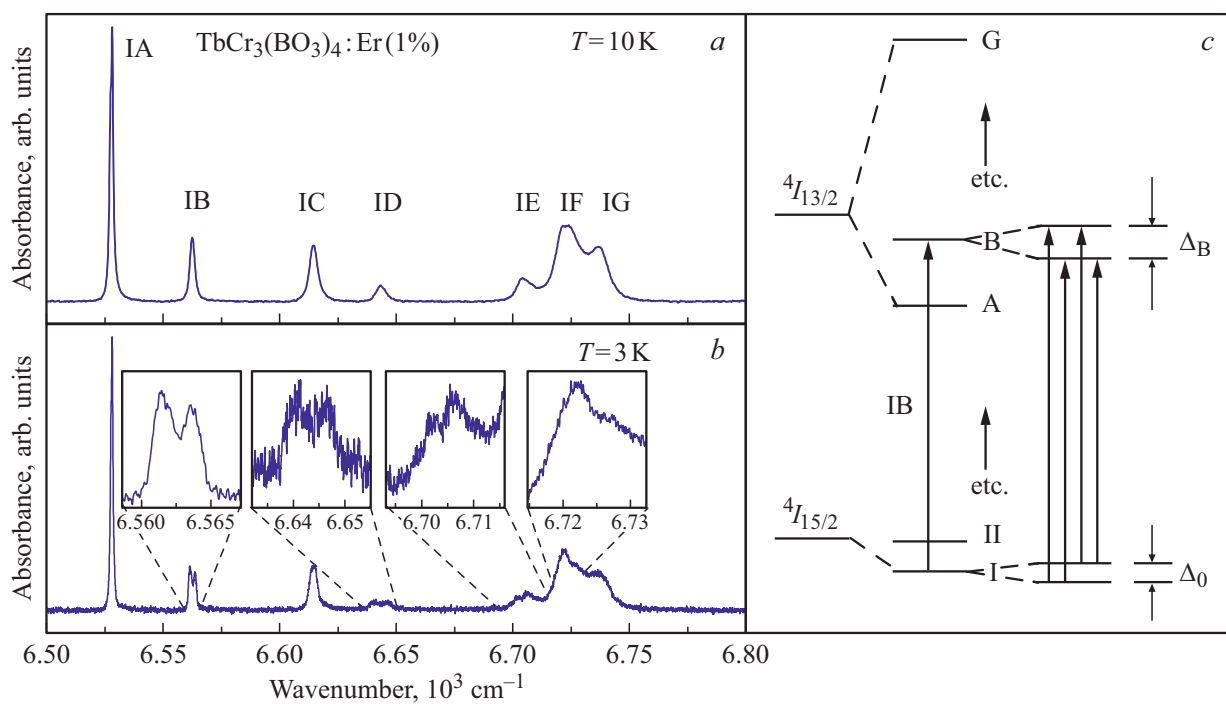
In the case of terbium-chromium borate, the magnetic phase transitions occur at temperatures below 10 K. Figure 5, *b* shows that four lines out of seven transitions  $^4I_{15/2} \rightarrow ^4I_{13/2}$  in the  $\text{Er}^{3+}$  ion in  $\text{TbCr}_3(\text{BO}_3)_4:\text{Er}(1\%)$  at low temperatures split into two components. Figure 6, *a* shows the line IA belonging to the spectral transition  $^4I_{15/2} \rightarrow ^4I_{13/2}$  in the  $\text{Er}^{3+}$  ion. This line is a doublet, and the doublet structure is also observed at temperatures well above the phase transitions. It appears that the doublet is associated with the presence of the monoclinic modification  $C2/c$ . The relative intensities of the doublet lines do not provide direct information on the relative number of rhombohedral and monoclinic modifications, since the strengths of the transition oscillators can differ significantly.

Figure 6, *b–d* shows the temperature dependences of the position of the center of masses, the half-width, and the intensity of the doublet line IA. All graphs have two features. At a temperature  $T_1 = 8.8 \text{ K}$ , which was compared on the basis of magnetic measurements with the antiferromagnetic ordering of the chromium subsystem in  $\text{TbCr}_3(\text{BO}_3)_4$  [46], a narrowing of the spectral line occurs (which leads to the peak intensity increasing), while no additional splitting is observed. A similar behavior was observed, for example, in the paper [63], where a sharp narrowing of the spectral lines  $\text{Sm}^{3+}$  in the RE francisite  $\text{Cu}_3\text{Sm}(\text{SeO}_3)_2\text{O}_2\text{Cl}$  occurred at the temperature of magnetic ordering of copper in the absence of these lines splitting. It appears that in these cases the magnetic structure arising in the subsystem of  $d$ -ions due to exchange interaction is such that the  $f-d$ -exchange (usually highly anisotropic) is small. It is  $f-d$ -exchange that determines the splitting of the spectral lines of RE ion in magnetically ordered crystal containing  $d$ - and  $f$  (RE)-ions. In paramagnetic phase the magnetic moments of  $d$ -ions fluctuate in magnitude and direction, which leads to fluctuating splitting of Kramers doublets of RE ions, and, as a result, to widening of the spectral lines [62]. This widening is removed by magnetic ordering of the crystal.

At the temperature  $T_2 = 5 \text{ K}$ , the narrowing of line IA is replaced by widening. In the paper [46] the phase transition observed at  $T_2 = 5 \text{ K}$  was presumably interpreted as spin-reorientational. Our data do not contradict this interpretation: the observed widening of the IA line can be associated with increased splitting of the Kramers doublets of the  $\text{Er}^{3+}$  ion with change in the orientation of the magnetic moments of the  $\text{Cr}^{3+}$  ions. In explicit form splitting is seen on the lines IB, ID, IE, IF of the transition  $^4I_{15/2} \rightarrow ^4I_{13/2}$  in the  $\text{Er}^{3+}$  ion. As the temperature decreases, these lines behave in the same way. As an



**Figure 4.** Absorption spectra of  $\text{TbCr}_3(\text{BO}_3)_4$  in paramagnetic (a), and also of  $\text{TbCr}_3(\text{BO}_3)_4:\text{Er}(1\%)$  in paramagnetic (10 K) and antiferromagnetic (3 K) (b) states in areas of transitions  ${}^7F_6 \rightarrow {}^7F_{2,1,0}$  in the  $\text{Tb}^{3+}$  ion. The insert shows the diagram of the energy levels of the  $\text{Tb}^{3+}$  ion, which explains the designations of the lines. The asterisk \* denotes satellites of the main lines due to lattice defects.



**Figure 5.** Absorption spectrum of the  $\text{Er}^{3+}$  ion in paramagnetic (a) and antiferromagnetic (b)  $\text{TbCr}_3(\text{BO}_3)_4:\text{Er}(1\%)$ ; diagram of energy levels of multiplets  ${}^4I_{15/2}$  and  ${}^4I_{13/2}$  of the  $\text{Er}^{3+}$  ion (c).

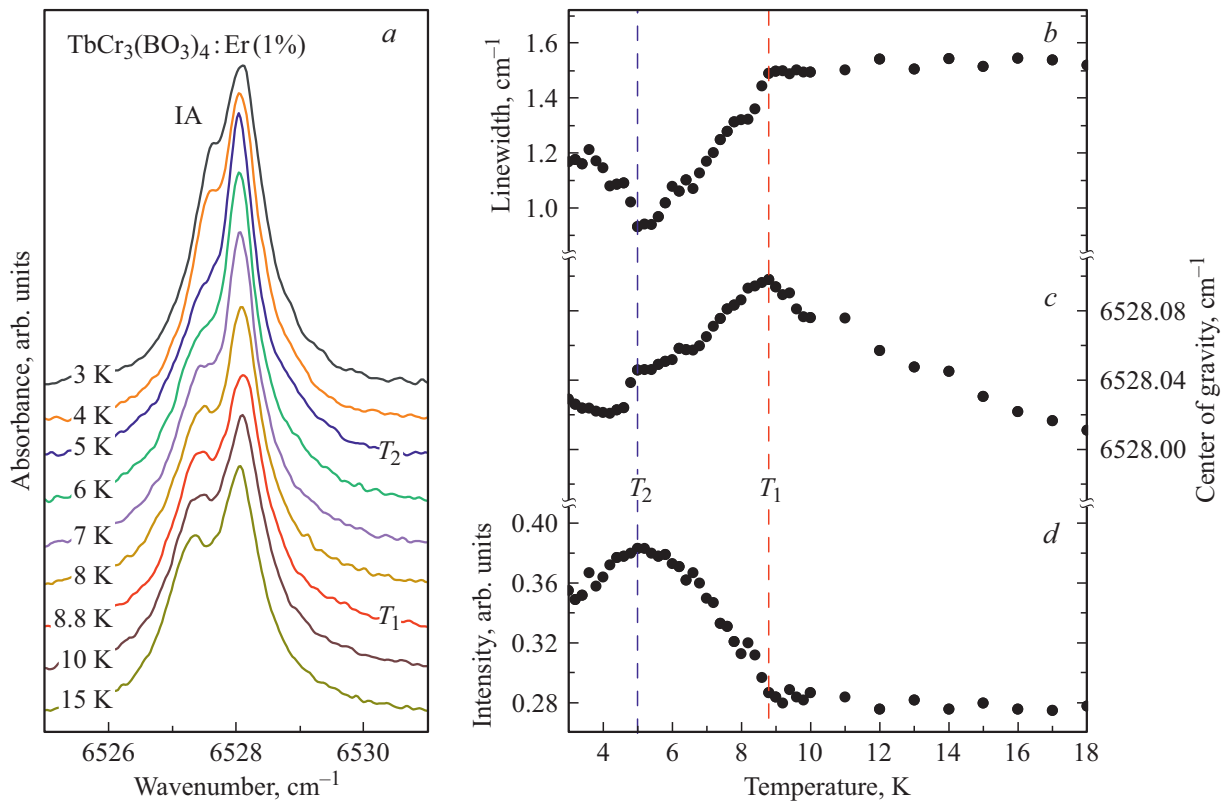


**Figure 6.** Absorption line IA of transition  ${}^4I_{15/2} \rightarrow {}^4I_{13/2}$  in the  $\text{Er}^{3+}$  ion in  $\text{TbCr}_3(\text{BO}_3)_4:\text{Er}(1\%)$  (a) and temperature dependencies of its half-width (b), positions of center of masses (c), intensities (d).

example, Fig. 7 shows the absorption line IB, as well as the temperature dependencies of its position and the magnitude of its splitting. It can be seen that the contour of the line does not change until 5 K, after which the line splits into two components.

The observed spectral dependences can be explained as follows. Since no splittings were found for the spectral lines at  $T_1$ , we can conclude that in the temperature range from  $T_1$  to  $T_2$  the energy levels of the ground and excited multiplets do not split. Since below  $T_2$  the spectral lines either widen or have two components whose relative intensities do not change with temperature decreasing, this can be attributed to a specific splitting scheme in which zero splitting is observed for the ground doublet (in this case, two of the four components coincide during magnetic ordering). Thus, the observed line splittings correspond to the splittings of the energy levels of the excited multiplet. For lines IB of the transition  ${}^4I_{15/2} \rightarrow {}^4I_{13/2}$  in the  $\text{Er}^{3+}$  ion the splitting at 3.0 K is  $2.1 \text{ cm}^{-1}$ , for line ID —  $5.7 \text{ cm}^{-1}$ , for line IE —  $4.9 \text{ cm}^{-1}$ , for line IF —  $6.7 \text{ cm}^{-1}$ .

The splitting of Kramers doublets in the middle field approximation is given by formula

$$\Delta_k = \sqrt{\sum (g_{ki} B_i)^2}, \quad (1)$$

where  $g_{ki}$  are  $i$ -th ( $i = x, y, z$ ) components of  $g$ -factors,  $B_i$  is magnetic field acting on  $k$ -th Kramers doublet. It can

be assumed that in the temperature range of  $T_1 > T > T_2$  the anisotropic  $g_{ki}$ -factor has close to zero  $i$ -component along the magnetic field  $B_i$ , and at temperature below  $T_2$  it already has a non-zero value. Since RE chromium borates are understudied at present, then additional studies are required to determine the nature of the transition  $T_2$ .

By comparison with ferroborate  $\text{TbFe}_3(\text{BO}_3)_4$ , terbium-chromium borate is ordered antiferromagnetically at more low temperature (8.8 K versus 41 K), has smaller values of splittings  $\Delta_B$  and  $\Delta_0$  for transition  ${}^4I_{15/2} \rightarrow {}^4I_{13/2}$  in the  $\text{Er}^{3+}$  ion —  $2.1 \text{ cm}^{-1}$  at 3.0 K versus  $5.0 \text{ cm}^{-1}$  at 4.5 K and  $0 \text{ cm}^{-1}$  at 3.0 K versus  $1.9 \text{ cm}^{-1}$  at 4.5 K, respectively [61]. This fact indicates a lower effective magnetic field in  $\text{TbCr}_3(\text{BO}_3)_4$  as compared to  $\text{TbFe}_3(\text{BO}_3)_4$ .

## Conclusion

The paper presents studies of growing conditions, structural features, and optical characteristics of terbium-chromium borate with the huntite structure. By the ratio of the intensities of the phonon modes  $\sim 71$  and  $\sim 81 \text{ cm}^{-1}$  the content of polytype modifications with sp.gr.  $R32$  and  $C2/c$  was estimated for further improvement of the growth method of  $\text{TbCr}_3(\text{BO}_3)_4$  crystals and to obtain single-phase compounds. The energies of the Stark levels

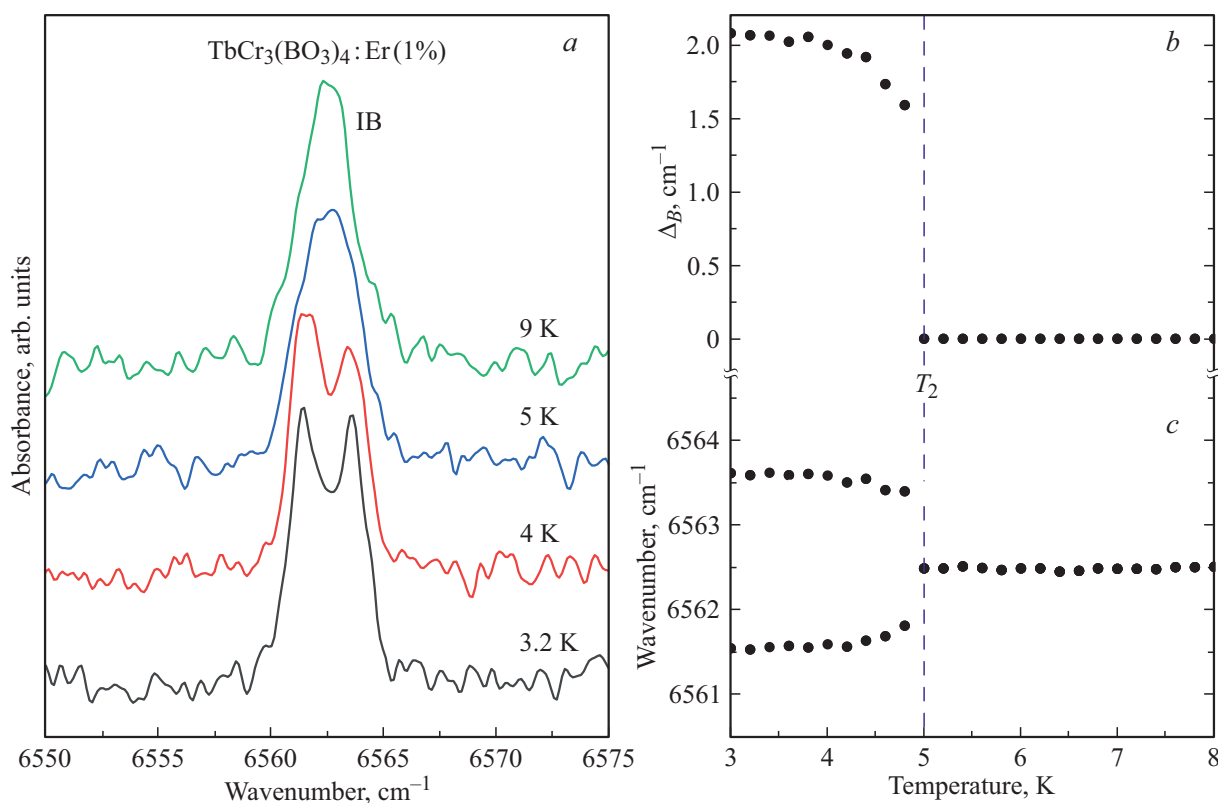


**Figure 7.** Low temperature absorption spectra of  $\text{TbCr}_3(\text{BO}_3)_4:\text{Er}(1\%)$  into region of spectral line IB of transition  ${}^4I_{15/2} \rightarrow {}^4I_{13/2}$  in the  $\text{Er}^{3+}$  ion in  $\text{TbCr}_3(\text{BO}_3)_4:\text{Er}(1\%)$  (a) and temperature dependencies of its splitting (b) and positions (c).

of this ion in the modification with pr.gr. R32 were determined from the temperature dependent absorption spectra of terbium-chromium borate in the range of electronic transitions in the  $\text{Tb}^{3+}$  ion. The temperature dependence of the absorption spectra of  $\text{TbCr}_3(\text{BO}_3)_4:\text{Er}(1\%)$  in the region of the transition  ${}^4I_{15/2} \rightarrow {}^4I_{13/2}$  in  $\text{Er}^{3+}$  probe ion confirmed the presence of two magnetic transitions in terbium-chromium borate previously established from magnetic measurements [46]. The spectroscopic data agree with the interpretation of phase transitions proposed in the paper [46]: at  $T_1 = 8.8$  K the chromium subsystem in  $\text{TbCr}_3(\text{BO}_3)_4$  is antiferromagnetically ordered, while at  $T_2 = 5$  K the magnetic moments of chromium are reoriented.

### Acknowledgments

The authors are grateful to M.N. Popova and S.A. Klimin for valuable comments on the manuscript.

### Funding

Experimental work on growing crystals of terbium-chromium borate was carried out at the expense of the Russian Science Foundation (project № 19-12-00235), spectroscopic studies were supported by the RSF grant № 19-12-00413.

### Conflict of interest

The authors declare that they have no conflict of interest.

### References

- [1] S. Trofimenko. *Chemical Reviews*, **93**(3), 943 (1993). DOI: 10.1021/cr00019a006
- [2] P. Becker. *Advanced Materials*, **10**(13), 979 (1998). DOI: 10.1002/(SICI)1521-4095(199809)10:13<979::AID-ADMA979>3.0.CO;2-N
- [3] C. Chen, Y. Wang, B. Wu, K. Wu, W. Zeng, L. Yu. *Nature*, **373**, 322 (1995). DOI: 10.1038/373322a0
- [4] C. Chen, G. Liu. *Ann. Rev. Materials Science*, **16**, 203 (1986). DOI: 10.1146/annurev.ms.16.080186.001223
- [5] M. Mutailipu, M. Zhang, Z. Yang, S. Pan. *Accounts Chem. Research*, **52**(3), 791 (2019). DOI: 10.1021/acs.accounts.8b00649
- [6] T. Sasaki, Y. Mori, M. Yoshimura, Y.K. Yap, T. Kamimura. *Science and Engineering: R: Reports*, **30**(1-2), 1 (2000). DOI: 10.1016/S0927-796X(00)00025-5
- [7] H. Huang, Y. He, Z. Lin, L. Kang, Y. Zhang. *J. Phys. Chem. C*, **117**(44), 22986 (2013). DOI: 10.1021/jp4084184
- [8] K.K. Shen, S. Kochesfahani, F. Jouffret. *Polymers for Advanced Technologies*, **19**(6), 469 (2008). DOI: 10.1002/pat.1119
- [9] R. Millini, G. Perego, G. Bellussi. *Topics in Catalysis*, **9**(1), 13 (1999). DOI: 10.1023/A:1019198119365
- [10] J.L.C. Rowsell, J. Gaubicher, L.F. Nazar. *J. Power Sources*, **97–98**, 254 (2001). DOI: 10.1016/S0378-7753(01)00532-8

- [11] F. Qin, R.K. Li. *J. Crystal Growth*, **318** (1), 642 (2011). DOI: 10.1016/j.jcrysgro.2010.08.037
- [12] G. Aka, A. Brenier. *Opt. Materials*, **22** (2), 89 (2003). DOI: 10.1016/S0925-3467(02)00351-8
- [13] S. Wang, E.V. Alekseev, J. Ling, G. Liu, W. Depmeier, T.E. Albrecht-Schmitt. *Chemistry of Materials*, **22** (6), 2155 (2010). DOI: 10.1021/cm9037796
- [14] E.R. Wang, J.H. Huang, S.J. Yu, Y.Z. Lan, J.W. Cheng, G.Y. Yang. *Inorganic Chemistry*, **56** (12), 6780 (2017). DOI: 10.1021/acs.inorgchem.7b00975
- [15] C. Chen, Y. Wu, R. Li. *Intern. Rev. Phys. Chem.*, **8** (1), 65 (1989). DOI: 10.1080/01442358909353223
- [16] C.F. Dewey, W.R. Cook, R.T. Hodgson, J.J. Wynne. *Appl. Phys. Lett.*, **26** (12), 714 (1975). DOI: 10.1063/1.88047
- [17] C. Chen, B. Wu, A. Jiang, G. You. *Science in China, Series B — Chemistry, Biological, Agricultural, Medical & Earth Sciences*, **28** (3), 235 (1985). DOI: 10.1360/yb1985-28-3-235
- [18] C. Chen, Y. Wu, A. Jiang, B. Wu, G. You, R. Li, S. Lin. *J. Opt. Soc. Am. B*, **6** (4), 616 (1989). DOI: 10.1364/JOSAB.6.000616
- [19] Y. Wu, T. Sasaki, N. Nakai, A. Yokotani, H. Tang, C. Chen. *Appl. Phys. Lett.*, **62** (21), 2614 (1993). DOI: 10.1063/1.109262
- [20] Y. Mori, I. Kuroda, S. Nakajima, T. Sasaki, S. Nakai. *Appl. Phys. Lett.*, **67** (13), 1818 (1995). DOI: 10.1063/1.115413
- [21] H. Hellwig, J. Liebertz, L. Bohatý. *Solid State Commun.*, **109** (4), 249 (1998). DOI: 10.1016/S0038-1098(98)00538-9
- [22] C.T. Chen, G.L. Wang, X.Y. Wang, Z.Y. Xu. *Appl. Phys. B*, **97**, 9 (2009). DOI: 10.1007/s00340-009-3554-4
- [23] Z. Guoqing, X. Jun, C. Xingda, Z. Heyu, W. Siting, X. Ke, D. Peizhen, G. Fuxi. *J. Crystal Growth*, **191** (3), 517 (1998). DOI: 10.1016/S0022-0248(98)00162-6
- [24] S. Zhang, X. Wu, Y. Song, D. Ni, B. Hu, T. Zhou. *J. Crystal Growth*, **252** (1–3), 246 (2003). DOI: 10.1016/S0022-0248(03)00867-4
- [25] M. He, X. Chen, Y. Sun, J. Liu, J. Zhao, C. Duan. *Crystal Growth & Design*, **7** (2), 199 (2007). DOI: 10.1021/cg0606141
- [26] Z. Jia, N. Zhang, Y. Ma, L. Zhao, M. Xia, R. Li. *Crystal Growth & Design*, **17** (2), 558 (2017). DOI: 10.1021/acs.cgd.6b01428
- [27] R.K. Li, Y.Y. Ma. *CrystEngComm*, **14**, 5421 (2012). DOI: 10.1039/C2CE25240F
- [28] X. Chen, B. Zhang, F. Zhang, Y. Wang, M. Zhang, Z. Yang, K.R. Poepplmeier, S. Pan. *J. Am. Chem. Society*, **140** (47), 1631 (2018). DOI: 10.1021/jacs.8b10009
- [29] Y. Huang, H. Chen, S. Sun, F. Yuan, L. Zhang, Z. Lin, G. Zhang, G. Wang. *J. Alloys and Compounds*, **646**, 1083 (2015). DOI: 10.1016/j.jallcom.2015.06.196
- [30] P. Dekker, J.M. Dawes, J.A. Piper, Y. Liu, J. Wang. *Opt. Commun.*, **195** (5–6), 431 (2001). DOI: 10.1016/S0030-4018(01)01347-5
- [31] B. Denker, B. Galagan, L. Ivleva, V. Osiko, S. Sverchkov, I. Voronina, J.E. Hellstrom, G. Karlsson, F. Laurell. *Appl. Phys. B*, **79** (5), 577 (2004). DOI: 10.1007/s00340-004-1605-4
- [32] A.M. Kadomtseva, Yu.F. Popov, G.P. Vorob'ev, A.P. Pyatakov, S.S. Krotov, K.I. Kamilov, V.Yu. Ivanov, A.A. Mukhin, A.K. Zvezdin, A.M. Kuz'menko, L.N. Bezmaternykh, I.A. Gudim, V.L. Temerov. *Low Temperature Physics*, **36** (6), 511 (2010). DOI: 10.1063/1.3457390
- [33] A.K. Zvezdin, S.S. Krotov, A.M. Kadomtseva, G.P. Vorob'ev, Y.F. Popov, A.P. Pyatakov, L.N. Bezmaternykh, E.A. Popova. *J. Experiment. and Theor. Phys. Lett.*, **81** (6), 272 (2005). DOI: 10.1134/1.1931014
- [34] A.K. Zvezdin, G.P. Vorob'ev, A.M. Kadomtseva, Y.F. Popov, A.P. Pyatakov, L.N. Bezmaternykh, A.V. Kuvardin, E.A. Popova. *J. Experiment. and Theor. Phys. Lett.*, **83** (11), 509 (2006). DOI: 10.1134/S0021364006110099
- [35] Y.F. Popov, A.P. Pyatakov, A.M. Kadomtseva, G.P. Vorob'ev, A.K. Zvezdin, A.A. Mukhin, V.Yu. Ivanov, I.A. Gudim. *J. Experiment. And Theor. Phys.*, **111** (2), 199 (2010). DOI: 10.1134/S1063776110080066
- [36] V.S. Kurazhkovskaya, E.A. Dobretsova, E.Y. Borovikova, V.V. Mal'tsev, N.I. Leonyuk. *J. Structural Chemistry*, **52** (4), 699 (2011). DOI: 10.1134/S0022476611040081
- [37] E.Y. Borovikova, E.A. Dobretsova, K.N. Boldyrev, V.S. Kurazhkovskaya, V.V. Maltsev, N.I. Leonyuk. *Vibrational Spectroscopy*, **68**, 82 (2013). DOI: 10.1016/j.vibspec.2013.05.004
- [38] K.N. Boldyrev, N.N. Kuzmin, E.A. Dobretsova. *Opt. Spectrosc.*, **129** (1), 41 (2021). DOI: 10.21883/OS.2021.01.50437.248-20 [K.N. Boldyrev, N.N. Kuzmin, E.A. Dobretsova. *Opt. Spectrosc.*, **129** (1), 37 (2021). DOI: 10.1134/S0030400X21010033]
- [39] A.N. Bludov, Y.O. Savina, V.A. Pashchenko, S.L. Gnatchenko, I.V. Kolodiy, V.V. Mal'tsev, N.N. Kuzmin, N.I. Leonyuk. *Low Temperature Physics*, **46** (6), 643 (2020). DOI: 10.1063/10.0001250
- [40] E.A. Popova, N.I. Leonyuk, M.N. Popova, E.P. Chukalina, K.N. Boldyrev, N. Tristan, R. Klingeler, B. Büchner. *Phys. Rev. B*, **76** (5), 054446 (2007). DOI: 10.1103/PhysRevB.76.054446
- [41] K.N. Boldyrev, E.P. Chukalina, N.I. Leonyuk. *Phys. Solid State*, **50** (9), 1681 (2008). DOI: 10.1134/S1063783408090187
- [42] Ł. Gondek, A. Szytuła, J. Przewoźnik, J. Żukrowski, A. Prokhorov, L. Chernush, E. Zubov, V. Dyakonov, R. Duraj, Yu. Tyvanchuk. *J. Solid State Chemistry*, **210** (1), 30 (2014). DOI: 10.1016/j.jssc.2013.10.029
- [43] A.N. Bludov, Y.O. Savina, V.A. Pashchenko, S.L. Gnatchenko, V.V. Mal'tsev, N.N. Kuzmin, N.I. Leonyuk. *Low Temperature Physics*, **44** (5), 423 (2018). DOI: 10.1063/1.5034153
- [44] A.N. Bludov, Y.O. Savina, M.I. Kobets, V.A. Pashchenko, S.L. Gnatchenko, N.N. Kuzmin, V.V. Mal'tsev, N.I. Leonyuk. *Low Temperature Physics*, **44** (5), 453 (2018). DOI: 10.1063/1.5034159
- [45] A. Bludov, Y. Savina, M. Kobets, V. Khrustalyov, V. Savitsky, S. Gnatchenko, T. Zajarniuk, A. Lynnyk, M.U. Gutowska, A. Szewczyk, N. Kuzmin, V. Mal'tsev, N. Leonyuk. *J. Magnetism and Magnetic Materials*, **512**, 167010 (2020). DOI: 10.1016/j.jmmm.2020.167010
- [46] N.N. Kuzmin, V.V. Maltsev, E.A. Volkova, N.I. Leonyuk, K.N. Boldyrev, A.N. Bludov. *Inorganic Materials*, **56** (8), 828 (2020). DOI: 10.1134/S0020168520080087
- [47] A.N. Bludov, Y.O. Savina, V.A. Pashchenko, S.L. Gnatchenko, T. Zajarniuk, A. Lynnyk, M.U. Gutowska, A. Szewczyk, I.V. Kolodiy, V.V. Mal'tsev, N.N. Kuzmin, N.I. Leonyuk. *Low Temperature Physics*, **46** (7), 697 (2020). DOI: 10.1063/10.0001367
- [48] E.A. Dobretsova, K.N. Boldyrev, M.N. Popova, V.A. Chernyshev, E.Y. Borovikova, V.V. Maltsev, N.I. Leonyuk. *J. Physics: Conference Series*, **737**, 012035 (2016). DOI: 10.1088/1742-6596/737/1/012035

- [49] E.L. Belokoneva, M.A. Simonov, A.V. Pashkova, T.I. Timchenko, N.V. Belov. *Doklady Akademii nauk SSSR*, **255** (4), 854 (1980) (in Russian).
- [50] V. Maltsev, E. Janod. *J. Crystal Growth*, **240** (1–2), 170 (2002). DOI: 10.1016/S0022-0248(02)00856-4
- [51] M.N. Popova, T.N. Stanislavchuk, B.Z. Malkin, L.N. Bezmaternykh. *J. Physics: Condensed Matter*, **24** (19), 196002 (2012). DOI: 10.1088/0953-8984/24/19/196002
- [52] L.N. Bezmaternykh, S.A. Kharlamova, V.L. Temerov. *Crystallography Reports*, **49** (5), 855 (2004). DOI: 10.1134/1.1803319
- [53] V.F. Zolin, L.G. Koreneva *Redkozemel'ny zond v khimii i biologii* (Nauka, Moskva, 1980) (in Russian).
- [54] G.G. Chepurko, I.V. Paukov, M.N. Popova, Ja. Zoubkova. *Solid State Commun.*, **79** (7), 569 (1991). DOI: 10.1016/0038-1098(91)90911-E
- [55] M.N. Popova, S.A. Klimin, R. Troć, Z. Bukowski. *Solid State Commun.*, **102** (1), 71 (1997). DOI: 10.1016/S0038-1098(96)00700-4
- [56] N.I. Agladze, G.G. Chepurko, M.N. Popova, E.P. Hlybov. *Phys. Lett. A*, **133** (4–5), 260 (1988). DOI: 10.1016/0375-9601(88)91028-6
- [57] I.V. Paukov, M.N. Popova, B.V. Mill. *Phys. Lett. A*, **169** (4), 301 (1992). DOI: 10.1016/0375-9601(92)90463-V
- [58] Yu.A. Hadjiiskii, I.V. Paukov, M.N. Popova, B.V. Mill. *Phys. Lett. A*, **189** (1–2), 109 (1994). DOI: 10.1016/0375-9601(94)90827-3
- [59] M.N. Popova, I.V. Paukov, Yu.A. Hadjiiskii, B.V. Mill. *Phys. Lett. A*, **203** (5–6), 412 (1995). DOI: 10.1016/0375-9601(95)00391-F
- [60] M.N. Popova. *J. Magnetism and Magnetic Materials*, **321** (7), 716 (2009). DOI: 10.1016/j.jmmm.2008.11.033
- [61] M.N. Popova, E.P. Chukalina, T.N. Stanislavchuk, L.N. Bezmaternykh. *J. Magnetism and Magnetic Materials*, **300** (1), e440 (2006). DOI: 10.1016/j.jmmm.2005.10.187
- [62] M.N. Popova. *J. Alloys and Compounds*, **275–277**, 142 (1998). DOI: 10.1016/S0925-8388(98)00292-8
- [63] K.V. Zakharov, E.A. Zvereva, M.M. Markina, M.I. Stratan, E.S. Kuznetsova, S.F. Dunaev, P.S. Berdonosov, V.A. Dolgikh, A.V. Olenev, S.A. Klimin, L.S. Mazaev, M.A. Kashchenko, Md.A. Ahmed, A. Banerjee, S. Bandyopadhyay, A. Iqbal, B. Rahaman, T. Saha-Dasgupta, A.N. Vasiliev. *Phys. Rev. B*, **94**, 054401 (2016). DOI: 10.1103/PhysRevB.94.054401